# Radiative trapping of electrons in intense, circularly polarized laser beams

J.G. Kirk

*Max-Planck-Institut für Kernphysik, Heidelberg, Germany*

The dynamics of electrons in intense laser beams is strongly influenced by radiation reaction, which can lead to the trapping of electrons on limit cycles in phase space. Recently [1], this phenomenon has been studied in a simplified field configuration consisting of two circularly polarized plane waves of arbitrary amplitude and opposite helicity. The equations of motion of classical electrodynamics, including radiation reaction, were used to locate limit cycles and perform a linear stability analysis. This was complemented by stroboscopic maps generated by numerical integration of the orbits. It was shown that stable limit cycles underlie simple attractors, and that an unstable limit cycle may, nevertheless, have a strange attractor in its immediate neighbourhood, leading to a concentration of electron orbits in phase space. Here, we extend these results by including strong-field QED effects, which are important in experiments using optical lasers with intensity $> 10^{22}\,\mathrm{W\,cm^{-2}}$.

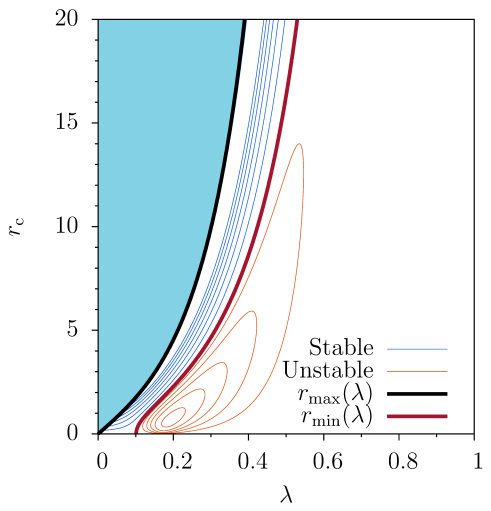


Figure 1: Growth/damping rates of limit cycles. Stable: blue contours, unstable: orange. Shaded region: no limit cycles [1].

In the chosen field configuration, the equations of motion of relativistic charged particles in classical electrodynamics, including radiation reaction, depend on only two parameters: the ratio $\lambda$ of the wave intensities and a radiation reaction parameter

$$r_c = 2e^2\omega/3mc^3\,(eE/mc\omega)^3 \approx 21\times I_{24}^{3/2}\lambda_{\mu\mathrm{m}}^2$$

where $\omega$ is the angular frequency of the two waves, and $E$, $I_{24}\times 10^{24}\,\mathrm{W\,cm^{-2}}$ and $\lambda_{\mu\mathrm{m}}\,\mu$m are the electric field amplitude, the intensity and the wavelength of the stronger of them (the "primary" wave). Limit cycles, which are in this case circles in the plane transverse to the direction of wave propagation, exist provided the radiation reaction term is not too strong. Their stability properties are shown in figure 1.

However, a classical treatment is adequate only when the electric field seen by the particle

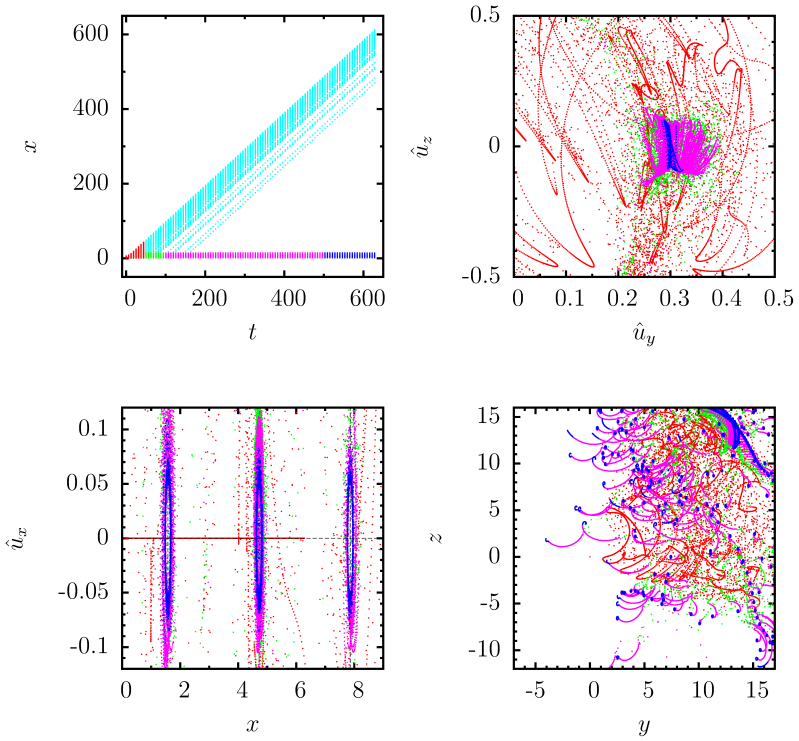


Figure 2: Stroboscopic plot for an unstable limit cycle, using classical electrodynamics with a reduction of the radiation reaction term due to QED effects. Parameters are $\lambda = 0.4$, $r_c = 0.5$, and $\eta_0 = 0.07$, corresponding to $\lambda_{\mu m} = 1$ and $I_{24} = 0.08$.

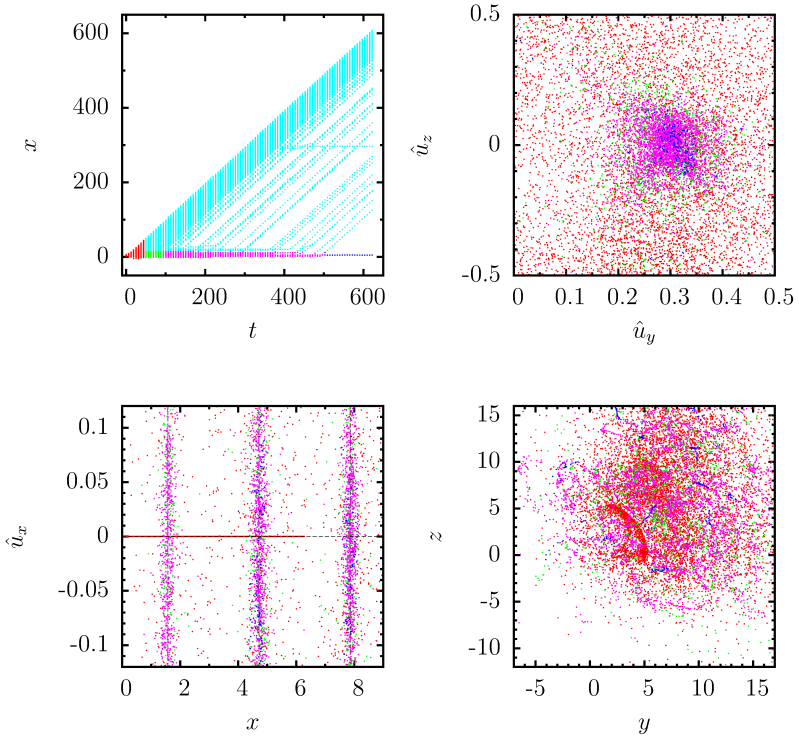


Figure 3: Stroboscopic plot for the same parameters as figure 2, but incorporating strong-field QED effects using a Monte-Carlo realisation of the trajectories.

in its rest frame is small compared to the Schwinger field. Unless the ratio, $\eta$, of these fields is negligibly small, a third parameter is needed to specify the dynamics, in addition to $\lambda$ and $r_c$. A convenient choice is

$$\begin{aligned}\eta_0 &= \left(\hbar\omega/mc^2\right)\left(eE/mc\omega\right)^2 \\ &\approx 0.89 \times I_{24}\lambda_{\mu\mathrm{m}}\end{aligned} \tag{1}$$

On a limit cycle, $\eta \approx \eta_0\,(1-\lambda)^2$, so that, for $\eta_0 \sim 1$, the classical radiation reaction force does not provide a good description. Two effects then come into play. Firstly, the rate at which energy is radiated is reduced — an effect analogous to the Klein-Nishina reduction of the Compton scattering cross section. Secondly, the discrete nature of the energy-loss process becomes apparent. The first effect can be incorporated into a classical treatment by applying an appropriate, $\eta$-dependent reduction to $r_c$[2]. The second requires a Monte-Carlo treatment of the trajectories [3].

The stroboscopic plots shown in figure 2 were constructed using the first approach with $\lambda = 0.4$ and parameters appropriate for a high-power optical laser of wavelength $1\,\mu$m and intensity $8 \times 10^{22}\,\mathrm{W\,cm^{-2}}$, in which case $\eta_0 \approx 0.07$. Trajectories of 5000 electrons were initiated at equally spaced points on the optical axis between $x = 0$ and $x = 2\pi$, with components of the four-velocity, normalized to $2eE/\omega$, of $\hat{u}_x = 0$, and $\hat{u}_y = \hat{u}_z = 1/\sqrt{2}$. Points depict the location in phase space at times $t = 2\pi n$ for $n = 0, 1, \ldots 200$. The top left panel shows the $t$-$x$ plane, with various colour codes that serve to identify the corresponding points in the other three panels. For $0 < t < 50$, points are shown in red. After roughly 50 wave periods, the trajectories separate into two groups: those that are picked up by the primary wave and acquire a high momentum in the positive $x$-direction (coloured light blue) and those that become trapped close to a limit cycle near the origin of the $x$-axis. The latter group is subdivided, as shown, according to the elapsed time. The remaining panels concentrate on the trapped particles. The top right panel plots the transverse components of the four-momentum, the bottom left panel a part of the $x$-$\hat{u}_x$ plane, close to the injection range, and containing three limit cycles, whose location (in the classical approximation) is marked by vertical dashed lines, and the lower right panel shows position in the transverse plane. This figure illustrates convergence onto the attractors, which have complex structure, and are located close to the (unstable) limit cycles.

Figure 3 shows the corresponding stroboscopic plots obtained from a Monte-Carlo implementation of QED effects. Although $\eta_0$ is relatively small, the differences between this figure and figure 2 are marked. In the QED case, attractors clearly retain their identity. However, as

can be seen from the upper left panel, particle trapping becomes less pronounced. The relatively large dispersion in $x$ of untrapped particles (light blue), which have relativistic velocity in the $x$ direction, indicates that these have escaped from an attractor after a prolonged period of trapping. Also, the horizontal structure seen in this panel at $x \approx 300$ illustrates that particles can be recaptured after a period of relativistic motion along $x$. Thus, for the chosen initial conditions, many more attractors are populated when QED effects are taken into account, and trajectories are never irreversibly either trapped or untrapped.

On the basis of purely classical calculations, it was suggest in [1] that the production of collimated MeV gamma-rays by inverse Compton scattering of the primary wave could be optimized by introducing a counter-propagating wave. The present results show that in the parameter range of figures 2 and 3, QED effects do not substantially modify this conclusion. However, further work is needed to quantify the dynamics in the parameter range $I_{24} > 0.1$, where a fully nonlinear electron-positron cascade is expected to develop.

## References

[1] J.G. Kirk, arXiv1605.00822, to appear in PPCF

[2] J.G. Kirk, A.R. Bell, I. Arka, PPCF 51, 085008 (2009)

[3] C.P. Ridgers, J.G. Kirk, R. Duclous, T.G. Blackburn, C.S. Brady, K. Bennett, T.D. Arber, A.R. Bell, J Comp. Phys. 260, 273 (2014)